

Organic Carbon Patterns and Budgets in the Long Island Sound Estuary

Penny Vlahos^{1*} and Michael M. Whitney¹

¹Department of Marine Sciences, University of Connecticut, Groton CT, USA

*P. Vlahos
Department of Marine Sciences
University of Connecticut
1080 Shennecossett Rd.
Groton, CT
06378, USA
Phone: 860-235-5337 (cell)
Email: penny.vlahos@uconn.edu

Running Header: Organic Carbon Patterns and Budgets in the LIS Estuary

This is the author manuscript accepted for publication and has undergone full peer review but has not been through the copyediting, typesetting, pagination and proofreading process, which may lead to differences between this version and the [Version record](#). Please cite this article as [doi:10.1002/lno.10638](https://doi.org/10.1002/lno.10638).

Abstract

A multi-year observational time series was evaluated across the 150 km central axis of the US east coast's Long Island Sound (LIS) estuary, in 3 distinct regions. Fluxes were calculated at the boundaries of the regions using observations coupled to a hydrodynamic model and applied to a mass balance to assess organic carbon (OC) export from LIS. For all years, during stratified summer periods, LIS was a net exporter of organic carbon to the continental shelf. LIS *annual* net carbon export however, varied with river flow. The heterotrophic or autotrophic nature of LIS also shifted inter-annually. During the mass balance analysis period (2009-2012), LIS ranged between net OC *import* from the continental shelf and heterotrophy in the lowest river flow year (2012) and net *export* of OC and autotrophy in the highest flow year (2011). Analysis suggests that LIS switches from net OC import to export when the annual river inputs exceed $19 \text{ km}^3 \text{ yr}^{-1}$. Applying these thresholds to the annual river flow record suggests that net import occurred in 15% of the last 20 years and that LIS usually is a net exporter of OC (85%). Annually averaged LIS carbon export values based on river flow conditions over the last 20 years are estimated at $56 \pm 64 \times 10^6 \text{ kg y}^{-1}$. Analysis also suggests that LIS shifts from net heterotrophic to net autotrophic when annual river flow exceeds $26 \text{ km}^3 \text{ yr}^{-1}$ (35% of the last 20 years). Net heterotrophic conditions are most common, representing 65% of the last 20 years.

Introduction

Estuaries are characterized by the differences in water chemistry across a freshwater to saline gradient. Increasing population in coastal regions, sea level rise and changes in freshwater inputs are leading to dramatic shifts in estuarine and coastal system biogeochemical balances. Organic matter (OM), both dissolved (DOC) and particulate (POC) flows from terrestrially loaded freshwaters as either a relatively refractory pool that will be further exported and as labile substrates that will be completely remineralized to CO₂ or partially remineralized to join the refractory pool (Walsh, 1995). In addition to DOC and POC, river waters and surface runoff carry ample nutrients that can stimulate *in situ* productivity adding to the total OM pool. The extent that estuaries rework existing OM loads or produce new OM (thus altering the OM pool) is characteristic of their geology and land use, climate (e.g. polar, temperate or tropical), changing freshwater inputs and water residence times (Macdonald et al., 2010, Jennerjahn et al., 2010). Longer residence times lead to more OM alteration and a more distinctly estuarine OM pool for export (Abril et al., 2002).

Aquatic systems are characterized as net autotrophic if they are a net OM source to surrounding systems (i.e. air and water) and net heterotrophic if they are a net OM sink. One approach to determining the net trophic condition of an estuary is by mass balance, comparing terrestrial OM loadings to net export (or import) to the shelf. The estuary is net autotrophic, neutral, or heterotrophic when export through the mouth exceeds, equals, or is less than terrestrial loading, respectively (Kemp et al., 1997, Vlahos et al., 2002, Najjar et al., 2010). Net autotrophy/heterotrophy occurs when *in situ* primary productivity is greater/less than sinks from

respiration and deposition. Thus, another approach to characterizing net autotrophy/heterotrophy is directly determining the *in situ* OM sources and sinks within the estuary (Vallino et al., 2005).

New estuarine production consumes inorganic carbon from the dissolved inorganic pool fueled by nutrient inputs and may subsequently lead to atmospheric carbon sequestration through the biological pump (Eppley and Peterson, 1979). The amount of inorganic carbon that is consumed through primary production (or released through respiration processes) is an important characteristic of coastal systems and is of particular interest in this current period of marine warming, particularly in areas of recently elevated warming rates (Seekell and Pace, 2011, Preston, 2008, Koutsikopoulos et al., 1998 Cook et al., 1998). The net drawdown of atmospheric CO₂ into an estuary *may* indicate net OM export to adjacent water bodies and/or net carbon burial in sediment while net release of CO₂ from an estuary *may* imply the area is a net sink for OM (Cai, 2011). As OM production and respiration are dynamically coupled processes, it is likely that the OM export status of estuaries, especially temperate ones, is seasonally altered. It is important to understand these shifts in OM export both spatially and temporally to constrain biogeochemically coupled cycles such as those of carbon (C) and nitrogen (N) in the midst of changing processes in estuaries driven by multiple pressures (Mitchell et al., 2015).

Long Island Sound (LIS) is a large urban estuary on the US East Coast with New York City bordering its western end. LIS's drainage basin (43,560 km²) is nearly 13 times its area (3420 km²), and the annual incoming fresh water is roughly 35% of the total volume (68 km³), (O'Donnell et al., 2014). The Connecticut River, the largest freshwater source (roughly 70%), enters near the LIS mouth (Figure 1). The Housatonic and several other rivers along the Connecticut coast also contribute to the terrestrial loading. The total load of OM from these

rivers has been estimated at $176 \times 10^6 \text{ kg y}^{-1}$ for 1988-1989 (NY DEC and CT DEP, 2000).

Hudson River waters enter LIS at its narrow western boundary via the East River (a tidal strait). Most of the exchange with the adjacent Mid-Atlantic Bight (MAB) shelf occurs through the LIS mouth at its eastern boundary. A smaller exchange with the MAB also occurs through the LIS head at the western boundary (through the East River connection). The western LIS experiences summertime hypoxia in its bottom waters (CT-DEEP, 2015) that has been linked to seasonal stratification and nutrient loads (Gobler et al., 2006). The estuary is characterized by long multi-month residence times (Gay and O'Donnell, 2009) that provide ample opportunity for OM alterations within the estuary. To date, LIS has not been characterized as a net source or sink of OM. The only estimates of net OM export from LIS have been reported for DOC by Buck et al., (2005) between $(140 \times 10^6 - 300 \times 10^6 \text{ kg y}^{-1})$ based on two sampling events in spring high river flow and summer low river flow periods of 2001. From the available loading and export estimates it is unclear whether LIS is net autotrophic or heterotrophic.

This study applies multi-year biogeochemical observations and hydrodynamic model results to characterize seasonal cycles and along-estuary patterns of organic C and N concentrations, C/N ratios of organic matter, and organic C transports. This information is combined with river loading estimates to calculate organic carbon budgets of the entire LIS, the western (WLIS), central (CLIS), and eastern (ELIS) regions. Net autotrophy or heterotrophy for each region is inferred from the carbon budgets. The results establish a vital baseline for organic C and N conditions in LIS and indicate uncertainties associated with inter-annual variability. The implications for the LIS ecosystem, future research, and environmental management also are discussed.

Methods

Concentrations

The Connecticut Department of Energy and Environmental Protection (CT-DEEP) has monitored water quality at stations throughout LIS since 1991 in support of the Long Island Sound Study (part of the U.S. Environmental Protection Agency National Estuary Program) (e.g. CT-DEEP 2015, Long Island Sound Study 1994) (Figure 1). The CT-DEEP database is accessible online at lisicos.uconn.edu. The year-round regularly sampled stations that are occupied once or twice each month are included in the present analysis. CT-DEEP analyzes near-surface and near-bottom water samples for carbon, nitrogen, phosphorus, silica, chlorophyll *a*, and suspended solids and collects corresponding water properties (salinity, temperature, dissolved oxygen, and pH). The present study focuses on the observed DOC, particulate carbon (PC), particulate nitrogen (PN), total dissolved nitrogen (TDN), and dissolved organic nitrogen (DON, calculated by subtracting ammonium, nitrite and nitrate concentrations from TDN). Nitrogen is selected to represent nutrient regimes because more loading data are available than for other nutrients (e.g. Varekamp et al., 2014), nitrogen-limitation of phytoplankton exists in LIS (Gobler et al., 2006), and water quality management has focused on nitrogen (e.g. New York State Department of Environmental Conservation and CT-DEEP, 2000). Note that the CT-DEEP dataset reports total particulate carbon and nitrogen as PC and PN and does not correct for inorganic carbon and nitrogen in the particulate matter though the inorganic carbon is usually small in these particles (<2%). PC is therefore used directly as a proxy for POC. The C/N ratio of dissolved OM is calculated as DOC/DON (in molar units). For this study, concentrations are

analyzed for an 8-year period spanning January 2008 through December 2014. Earlier observations from 1995 to 2007 are not used because of DOC data quality concerns. The DOC values and C/N ratios prior to 2008 are often unrealistically high for this system. All time periods used in relevant to this study are summarized in Table S1 for convenience.

The strengths of the CT-DEEP water quality dataset are the spatial coverage along the estuary and the multi-year record length. Weaknesses include the limited vertical and lateral resolution. The sampling frequency also cannot resolve weekly, daily, or tidal variability. The inability to fully resolve the spatial and temporal variability introduces an unknown amount of uncertainty around concentrations intended to represent monthly to inter-annual variability. Error bars presented in this paper do not represent this error, but rather show the standard deviation assessing the inter-annual variability of the monthly or annual values. Estimates of the uncertainty introduced by not fully resolving spatial and temporal variability are included in the Results and Discussion.

Fluxes

Export and import through LIS boundaries are constrained by calculating advective fluxes (or transports) through adjacent regions. Calculating advective fluxes of carbon and nutrients requires velocity information not included in the CT-DEEP database. This analysis relies on velocities from an existing hydrodynamic model of LIS (Whitney et al., 2016). It is an application of the Regional Ocean Modeling System (ROMS, Haidvogel et al., 2008) for the LIS, Block Island Sound, and adjacent continental shelf. Horizontal resolution within LIS is 0.5-1 km and vertical variations are resolved by 20 evenly-distributed vertical levels. Model forcing includes tides (applied along the shelf open boundaries), river discharge (applied at the tidal head

of each river), spatially-uniform wind stress, and spatially-uniform shortwave and downwelling longwave surface heat fluxes. Model performance has been evaluated relative to observations of tidal elevations, tidal currents, tidal-averaged salinities, and tidal-averaged velocities. Whitney et al., (2016) include a detailed description of model settings, observational comparisons, and analysis of model results. The 4-year analysis period spanning 2009 to 2012 for the prior research is used for fluxes in this study (that is, 4 of the 7 years of observations (2008 to 2014) are modelled for fluxes).

Advective fluxes are calculated for estuary cross sections at the LIS estuary head, between WLIS and CLIS regions, between CLIS and ELIS regions, and near the mouth (Figure 1). These cross sections are oriented north/south and pass through CT-DEEP stations A4, F3, J2, and K2. The outermost station, M3, is not used because this mouth boundary includes three segments separated by islands and it is unlikely that biogeochemical observations from one location can adequately represent conditions through each pass. The selected near-mouth cross section through K2 has no island interruptions and is east of the Connecticut River mouth. For each cross section, the volume fluxes per grid cell and vertical layer are used. These cell-layer volume fluxes (flowing through the cross section) are averaged over four semi-diurnal lunar (M_2) tidal cycles to create 4-year time series with a regular 2.07 day interval. The organic carbon observations have to be spatially interpolated and extrapolated to provide information for the entire cross section. A linear-interpolation approach is a straightforward way to proceed when the actual spatial variability is unknown. For the cross section between WLIS and CLIS, stations F2 and F3 are averaged together. Concentrations are taken as constant (at the near-surface sample value) from the surface down to the near-surface depth (approximately 2 m), linearly interpolated between the near-surface and near-bottom sample depths, then held constant (at the

near-bottom sample value) down to the deepest depth of the cross section. This concentration profile is used to interpolate to the vertical layers in each grid cell along the cross section; thus contours of the interpolated concentration field are horizontal. It is likely that there is considerable lateral variability in concentrations (e.g. Gobler et al., 2006; Whitney et al., 2016) that the CT-DEEP database and this analysis cannot resolve; this is one reason why the resulting fluxes are only estimates. The spatially interpolated concentration fields (available once or twice a month) are linearly interpolated to the 2.07 time interval of the cell-layer volume flux time series. These spatially and temporally interpolated concentrations are multiplied by the cell-layer volume fluxes and summed vertically through the water column and horizontally across to calculate the net carbon advective fluxes through each cross section. These net fluxes are used in the organic carbon budgets for each LIS region (described below). It is important to note that the net fluxes reflect the imbalance between larger opposing fluxes through each section associated with strong estuary exchange flow in this weakly stratified estuary (e.g. Whitney et al., 2016). It is also worth noting that correlations between tidal variations in concentrations and velocities (e.g. tidal pumping, MacCready 2004) can lead to net fluxes. The present approach misses this latter flux generation mechanism because the CT-DEEP dataset does not include sampling through a tidal cycle. It is likely that this missed influence grows stronger towards the mouth as the tidal currents increase (e.g. Whitney et al., 2016). As mentioned above, CT-DEEP observations do not partition PC into organic and inorganic parts; therefore POC fluxes are calculated using PC as a proxy for POC concentrations.

Estuary storage

The organic carbon masses in WLIS, CLIS, ELIS, and the entire budgeted LIS are calculated by multiplying the time-varying water volume in each region by the corresponding time-varying spatially averaged carbon concentrations. The time-varying volume is calculated from model results between the bounding across-estuary regions; the volume is the spatial integral of the sum of the bathymetry and the time-varying tidal-averaged surface elevation. The spatially averaged concentration for organic carbon in each region is calculated by averaging all near-surface and near-bottom samples from all stations within the region including those on bounding cross sections. The spatial averaged concentrations then are linearly interpolated to the same 2.07 time interval as the model results. Corresponding time rates of change are calculated as centered differences and indicate organic carbon storage rates when positive.

River Loadings

Loading from each river is calculated by multiplying river flow rates (or discharge) by carbon concentrations. The discharge time series for each river are based on observations from USGS stream gages (Whitney et al., 2016). Carbon data for the Connecticut and Housatonic Rivers were obtained from the USGS (Mullaney, 2016) for the years 2009 to 2012. Due to the sparsity of data, river DOC and POC (calculated by subtracting DOC from reported total organic carbon) values are binned by calendar month to obtain a monthly time series that could be coupled to monthly river flow rates as inputs into LIS used to calculate a seasonally resolved, annual mass balance (Figure S1). The annual concentration cycle applied to each river is interpolated to the corresponding discharge time series to calculate DOC and POC loads. POC ranges between 5 - 20% of the total organic carbon pool in these rivers and it is therefore important to consider both pools as separate inputs. Also the fate and transport of DOC and POC can be significantly

different as DOC is expected to be advected considerably further away from its source. The annual concentration cycle applied to each river is interpolated to the corresponding discharge time series to calculate DOC and POC loads. The Connecticut River represents over 70% of the freshwater flow into the LIS control volume. The Housatonic represents roughly another 15%. The remaining small rivers where organic carbon measurements are unavailable collectively account for only 15% of the freshwater inflow. Estimation of DOC and POC inputs from these smaller rivers is accomplished using their discharge and Housatonic concentrations that approximate actual smaller river concentrations to a degree sufficient for this budget analysis. Future work to improve the resolution of variations in smaller rivers is underway.

Budgets

Organic carbon budgets are obtained for each LIS region using the advective fluxes across the bounding cross sections (import and export), temporal changes in carbon mass (storage rates) within the LIS region, and direct river loading from tributaries (calculated as described above). Note that loading from the Hudson River (via the East River connection) is included in the western LIS boundary fluxes. The residual differences that complete the organic carbon budgets are attributed to the net effects of *in situ* production (P), respiration (R) and benthic sinks or sources (B). The residual term also includes the sum of any errors (ϵ) in each constrained term. The organic carbon mass budget for each LIS region can be expressed as:

$$\underbrace{\frac{d\bar{C}V}{dt}}_{\text{Storage rate}} = \underbrace{-\iint [C\vec{u} \cdot \hat{n}] dA_W - \iint [C\vec{u} \cdot \hat{n}] dA_E}_{\text{Advective flux (import and export)}} + \underbrace{+C_R Q_R}_{\text{River loading}} + \underbrace{+(P - R - B + \epsilon)}_{\text{"Net production"}} \quad (1)$$

In this equation, $\bar{C}V$ is the DOC or POC mass in the region, C signifies the DOC or POC concentrations at the boundaries, $\vec{u} \cdot \hat{n}$ indicates the outward normal velocities passing through the boundaries, A_W and A_E are the cross-sectional areas of the western and eastern boundaries,

C_R is the river concentration, Q_R is the river discharge, and the other symbols are defined above. Evaporative losses and organic carbon fluxes through the air-sea interface are assumed to be small and are folded into ϵ . The “net production” term in Equation (1) is solved as the residual after constraining the other terms. Negative advective flux indicates net export and a positive net production term indicates net autotrophic conditions. Fluxes are combined to calculate the DOC and POC budgets for each region and each year.

Results and Discussion

General Trends

CT-DEEP time series for station A4 in WLIS are shown in Figure 2. Since January 2008, DOC has remained relatively stable from year to year at $2.1 \pm 0.2 \text{ mgL}^{-1}$ ($175 \pm 16 \text{ }\mu\text{ML}^{-1}$) and $1.9 \pm 0.3 \text{ mgL}^{-1}$ ($158 \pm 25 \text{ }\mu\text{ML}^{-1}$) for surface and bottom waters respectively. The concentrations given after the “ \pm ” symbol in this paragraph indicate the temporal standard deviation of the corresponding time series. PC values (assumed to be a proxy for LIS POC) are $0.7 \pm 0.4 \text{ mgL}^{-1}$ in bottom waters and consistently higher in surface waters at $1.0 \pm 1.0 \text{ mgL}^{-1}$, typically peaking in July. Surface values are above near-bottom values from February to September for both DOC and PC as stratification and productivity increase, limiting vertical mixing. At station F2 (Figure S2) in CLIS the DOC concentrations are $1.8 \pm 0.2 \text{ mgL}^{-1}$ ($150 \pm 16 \text{ }\mu\text{ML}^{-1}$) and $1.7 \pm 0.3 \text{ mgL}^{-1}$ ($140 \pm 16 \text{ }\mu\text{ML}^{-1}$) in surface and deep waters. PC also drops to $0.6 \pm 0.3 \text{ mgL}^{-1}$ and $0.4 \pm 0.2 \text{ mgL}^{-1}$ in surface and deep samples. As with the WLIS there is a seasonal PC peak, but it is shifted to August and is more modest at 1.2 mgL^{-1} . At station K2 in ELIS (Figure S3) the seasonal change is smaller. DOC concentrations average $1.6 \pm 0.3 \text{ mgL}^{-1}$ ($130 \pm 16 \text{ }\mu\text{ML}^{-1}$) and $1.5 \pm 0.3 \text{ mgL}^{-1}$ ($125 \pm 16 \text{ }\mu\text{ML}^{-1}$) for surface and bottom waters respectively and PC averages at

$0.4 \pm 0.1 \text{ mgL}^{-1}$ and $0.4 \pm 0.2 \text{ mgL}^{-1}$ in both surface and bottom waters respectively. There is only a slight peak in PC between June and August at 0.8 mgL^{-1} .

Annually, distinct along-estuary gradients (from west (head) to east (mouth)) are evident in the DOC and PC concentrations, averaged over the 2008-2014 period in Figure 3 a, b. Note that seasonal variations are removed through averaging. DOC concentrations decrease from west to east across the 12 CT-DEEP stations. Near-surface and near-bottom DOC concentrations at the westernmost station (A4) are 2.05 ± 0.05 to $1.47 \pm 0.04 \text{ mgL}^{-1}$ and 1.89 ± 0.09 to $1.38 \pm 0.02 \text{ mgL}^{-1}$, respectively. The concentrations given after the “ \pm ” symbol in these annual averages indicate the inter-annual standard deviation of the average values presented in the along-estuary trends (Figure 3). West to east DOC gradients along the 150 km central axis equate to a decrease of $0.003 \text{ mgL}^{-1}\text{km}^{-1}$ ($r^2 = 0.90$) for both surface and bottom waters. PC average concentrations (a proxy for POC) range from 1.01 ± 0.21 to $0.33 \pm 0.03 \text{ mgL}^{-1}$ from west to east in surface waters and 0.68 ± 0.10 to $0.32 \pm 0.02 \text{ mgL}^{-1}$ in deep waters. The PC gradient for near surface and deep waters are $0.004 \text{ mgL}^{-1}\text{km}^{-1}$ ($r^2 = 0.78$) and $0.001 \text{ mgL}^{-1}\text{km}^{-1}$ ($r^2 = 0.32$) respectively. The along-estuary patterns confirm a consistently higher surface PC (and by extension POC) over deep waters in WLIS and CLIS and vertically homogeneous values in ELIS.

DON, PN and TDN time series for station A4 in WLIS are illustrated in Figure 2 (c, d and e) over the same time period. As is the case for DOC there are significant seasonal trends. Surface DON, PN and TDN (0.20 ± 0.05 , 0.17 ± 0.17 , $0.42 \pm 0.19 \text{ mgL}^{-1}$) are higher than concentrations in deep waters (0.17 ± 0.05 , 0.10 ± 0.06 , $0.36 \pm 0.15 \text{ mgL}^{-1}$) in all cases. DON and PN both peak between June to August and experience the greatest divergence between surface to bottom concentrations during this period of productivity and stratification. Values converge in

September through January. The PN surface to bottom difference is double the corresponding DON difference. TDN has a different seasonal profile where surface to bottom differences are negligible between February to September when productivity is high and nutrients are relatively depleted. The TDN concentrations in this period are close to the DON concentrations. The surface is enriched between September to January and the DON can account for roughly 40% of the TDN pool suggesting inorganic N pools are not depleted. These patterns weaken towards the east. At station F2 in CLIS (Figure S2 c through e) the DON, PN seasonal profiles are similar to WLIS though TDN is lower (0.16 ± 0.03 , 0.08 ± 0.04 , $0.21 \pm 0.07 \text{ mgL}^{-1}$) in surface and bottom. Surface and deep TDN profiles are close throughout the season though DON accounts for all the TDN in the spring summer averages and roughly 60% in the fall winter periods. At station K2 in ELIS (Figure S3 c through e), seasonal variations do not appear significant. DON, PN and TDN ranges are similar in surface and deep waters at 0.13 ± 0.04 , 0.06 ± 0.02 , $0.19 \pm 0.05 \text{ mgL}^{-1}$ respectively.

The along-estuary DON and PN concentrations are shown in Figure 3 c and d. DON and PN in surface waters range from $0.20 \pm 0.13 \text{ mgL}^{-1}$ and $0.16 \pm 0.05 \text{ mgL}^{-1}$ respectively. Surface water concentrations are greater than bottom water concentrations in WLIS by 0.03 and CLIS by 0.05 mgL^{-1} , but converge in the ELIS. Surface TDN (Figure 3 e) ranges between 0.44 to 0.18 mgL^{-1} from west to east. Surface and bottom waters are similar throughout with some evidence of surface intensification at the western end. The inter-annual ranges however are large and therefore these slight differences are not significant. The largest along-estuary gradients of nitrogen pools are in the WLIS. For TDN, the maximum WLIS gradient is 3×10^{-4} and $7 \times 10^{-4} \text{ mgL}^{-1} \text{ km}^{-1}$ for near surface and deep waters, respectively. Eastward from station D3, TDN

gradients for near surface and deep waters are $4 \times 10^{-4} \text{ mgL}^{-1} \text{ km}^{-1}$ ($r^2 = 0.82$) and $5 \times 10^{-4} \text{ mgL}^{-1} \text{ km}^{-1}$ ($r^2 = 0.98$) respectively.

The C/N ratio of the dissolved OM (calculated as DOC/DON) is used as a proxy to assess the quality of the OM exchanged in LIS. At station A4 in WLIS (Figure 2 f), C/N ratios are 13 ± 3 and 14 ± 4 for surface and deep waters throughout the year. These ratios are somewhat higher for the CLIS (14 ± 3) and ELIS (16 ± 8). Annual averages (Figure 3 f) show a weak increasing trend in C/N ratios from west to east in surface waters. This is consistent with an input of low C/N ratio OM in the west, likely due to *in situ* primary productivity stimulated by nutrient loads that shift the ELIS as OM is reworked and mixed with significant OM inputs from Housatonic River in the CLIS and the Connecticut River in the ELIS.

Budgets

By coupling the CT-DEEP concentrations to the LIS model (as described in the methods), along-estuary fluxes of DOC and POC are estimated for LIS transects (note: POC \sim PC). These fluxes are combined with river loading and storage changes to estimate regional DOC and POC budgets for the WLIS, CLIS and ELIS regions (following Equation 1 as described in the Methods).

Figure 4a represents the LIS budget for OC during a low river flow year (2012). River loads increase from west to east for both DOC and POC because of the Housatonic River in CLIS and the larger Connecticut River in ELIS. Total river loads are $62.9 \times 10^6 \text{ kg y}^{-1}$; 72% is from the Connecticut River. Advective fluxes show the magnitude and direction of DOC and POC flows between regions. In WLIS, more DOC leaves westward than enters through its eastern boundary and from river loading (a smaller contributor). This net export contributes to the larger annual decrease in DOC mass storage ($-2.2 \times 10^6 \text{ kg y}^{-1}$) within WLIS. This larger storage decrease also

implies a loss due to a net *in situ* loss (by respiration and burial) of DOC of $1.4 \times 10^6 \text{ kg y}^{-1}$ that is at least 21% of the individual advective transports and twice the difference between advective transports and river loading. In WLIS POC is advected in from the East River and increases, resulting in a larger POC export to the adjacent CLIS. This net POC export implies a significant net production term of $1.5 \times 10^6 \text{ kg y}^{-1}$ since the river loading and storage change terms are small. Budgets for CLIS imply that CLIS exports DOC to both the WLIS and ELIS. The combined export is smaller than contributions from river loading and storage increases in CLIS. This imbalance implies a net DOC sink of $2.5 \times 10^6 \text{ kg y}^{-1}$ for CLIS. The POC import, river loading, and storage increases collectively imply a large net sink for POC consuming $9.2 \times 10^6 \text{ kg y}^{-1}$ in CLIS. Finally the ELIS is a net sink for both DOC and POC consuming a combined $64.8 \times 10^6 \text{ kg y}^{-1}$. Under these low river flow conditions the ELIS imports both DOC and POC from offshore waters. As a whole the LIS is net heterotrophic consuming $67.3 \times 10^6 \text{ kg y}^{-1}$ OC the majority of which occurs in the east and imports both DOC ($6.0 \times 10^6 \text{ kg y}^{-1}$) and POC ($4.7 \times 10^6 \text{ kg y}^{-1}$) through its boundaries. It is important to note that OC delivered to LIS from rivers may still be exported to the MAB, particularly the refractory material, even though there is a net import.

Freshwater residence (or flushing) times, calculated as the total freshwater volume in LIS (determined from annually averaged ROMS salinity fields), divided by the annual river discharge between 2009-2012 (the modeled period), range from 3.3 months in the highest flow year (2011) to as long as 6.2 months in the lowest flow year (2012). Higher river flowrates also intensify the degree of stratification and this *may* facilitate faster export of materials confined to the upper stratified layer. In low flow years, riverine OM likely experiences longer exposure for transformation prior to export. Nutrients delivered in low flow years are reduced and the labile *in*

situ production they stimulate is more likely to be respired with longer residence times. The slightly higher C/N ratio in ELIS in low flow years (e.g. 2012 in Figure 2f) is consistent with this explanation (consistent with selective removal of nitrogen by bacteria from DON and more re-worked material, see Hopkinson et al., 1997) though C/N variability is high and thus this can be inferred but not confirmed at this sampling resolution. Differences in high and low flow years may reveal important hints for the timescales involved in estuarine production, respiration and transformation that determine the nature of OC exported and possibly the intensity of hypoxia.

Figure 4b illustrates the budget in a high river flow year (2011) where carbon and nutrient inputs from tributaries are significantly higher. Total carbon inputs are $137.7 \times 10^6 \text{ kg y}^{-1}$, 68% of this is from the Connecticut River. Here the WLIS produces both DOC and POC, exporting DOC in both directions and POC eastward to the CLIS. The CLIS is relatively balanced for DOC with a slight net sink of $0.7 \times 10^6 \text{ kg y}^{-1}$ though it remains a significant sink for POC at $15.1 \times 10^6 \text{ kg y}^{-1}$. The ELIS is the region most influenced by these high flow conditions. There is a significant amount of DOC produced and there is a large net export of carbon due to the river loading, net production, and additions from the CLIS. Under these high flow conditions the LIS is net autotrophic producing a net $55.5 \times 10^6 \text{ kg y}^{-1}$. LIS exports $179.2 \times 10^6 \text{ kg y}^{-1}$ OC (98.6%) offshore through the ELIS mouth and a modest $2.6 \times 10^6 \text{ kg y}^{-1}$ OC (1.4%) through the narrow western boundary. Again it is the river loading and productivity of the ELIS that dominates the balance which merits higher resolution studies in this region.

In order to appreciate the seasonal contributions to the overall *in situ* production or loss of OC, the *in situ* term was evaluated separately for both low and high flow years. Figure 5a combines all three regions into a single LIS term in the center of the flow diagram and the seasonal

contributions from which the annual average is derived. Under low flow conditions the LIS remains a net sink for OM throughout the year with a net DOC sink in all seasons and a net POC sink in all seasons except spring. Under high flow conditions (Figure 5b) LIS is a net source of OC dominated by inputs in the winter, spring and summer and only the fall remains as a period of net consumption.

Relationships with Freshwater Inputs

The relationship between river flow and carbon export to the MAB is further investigated by comparing total DOC export to the MAB for 2009 to 2012 when complete budgets were calculated (Figure 6 a). LIS imports carbon from the adjacent MAB for years with river discharge below approximately $18.8 \text{ km}^3 \text{ y}^{-1}$ and exports carbon during higher discharge years. The relationship between river flow and the inferred net production with LIS for budget years is shown in Figure 6 b. The net trophic status of LIS changes when the annual average flow rates of the rivers combine to over $26.1 \text{ km}^3 \text{ y}^{-1}$. This occurs during periods when freshwater residence times are on the low end (3.3 months). Shifts in trophic status related to freshwater residence times in LIS may help constrain LIS *in situ* productivity and respiration timescales. At a three month freshwater residence time timescale, *in situ* production outpaces respiration. At a six month freshwater residence time, respiration significantly outpaces *in situ* production. This result may be a valuable consideration for future attempts to understand and predict the extent of bottom water hypoxia.

The long term record of total river flow into LIS from 1929-2015 is plotted in Figure 7. Also shown on this time series are the estimated threshold for export vs. import from the MAB and the threshold for transitioning from net auto to heterotrophy. This suggests that, for just over half of these years (53%), LIS is heterotrophic and a net exporter of OM to the MAB. From Figure 7 it is apparent that many of the highest flow years have occurred in recent decades. This increase in the mean river flow implies a shift in frequency of occurrence of net autotrophic conditions. Over the entire time series since 1929, LIS has river flows that meet the autotrophic, exporting criteria only 23% of the time. In the last 20 years (1996-2016), however, these conditions are met 35% of the time. This trend is consistent with other estuarine freshwater flows globally and worthy of future attention (Mitchell et al., 2015). Net export reversal at ELIS with the MAB occurs 24% of the time over the entire time series and only 15% of the time over the last 20 years, therefore LIS has been a net exporter of OC to the MAB 85% of the time since 1996. This result can be useful to estimate future carbon export to the MAB under different precipitation and regional climate scenarios. Though clearly the actual amount of DOC exported varies widely based on the above criteria, a weighted average export to the MAB since 1996 is estimated as $56 \pm 64 \times 10^6 \text{ kg y}^{-1}$, with a minimum of $-6 \times 10^6 \text{ kg y}^{-1}$ and maximum of $+175 \times 10^6 \text{ kg y}^{-1}$.

Errors

As mentioned in the Methods, the CT-DEEP water quality dataset cannot fully resolve all the spatial and temporal variability in LIS. The results presented can be combined with additional information to scale the uncertainty that may be introduced by not resolving tidal and lateral variability. As tidal currents progress through flood and ebb, water and its C and N concentrations sweep by a sampling station from the east and west, respectively. Horizontal tidal

excursions (during ebb or flood) increase from approximately 5 km in WLIS to 13 km in ELIS at the surface and from 3 to 5 km from west to east at the bottom (Bennett et al., 2010). Combining the tidal excursions with the long-term-average along-estuary DOC trends (Figure 3) indicates that the standard deviation of tidal variability introduces up to a 2% relative error in WLIS and CLIS. Up to a 7% uncertainty is estimated for ELIS because of the larger tidal excursions and lower concentrations. PC (and POC) gradients are proportionally larger than DOC gradients; consequently tidal variability can introduce up to a 7% relative error in WLIS, 6% in CLIS, and 15% in ELIS. These estimates indicate the uncertainty introduced by not resolving tidal variability is several times smaller than the standard deviations associated interannual variability (shown as error bars in Figure 3). Lateral variability also is unresolved in most areas, but stations H2, H4, and H6 are aligned across CLIS. Comparing the range of the long-term-average values at each station to the three-station mean value gives a sense of uncertainty introduced by lateral variability. Half the ranges for near surface and near bottom DOC are 3% and 2% of the corresponding three-station mean values. The lateral spread of PC (and POC) is larger. Half the ranges for near surface and near bottom POC are 7% and 12% of the corresponding three-station mean values. It appears that tidal and lateral variations introduce a comparable amount of uncertainty in CLIS. A current observational study by the authors will resolve the lateral and tidal variability of carbon and nutrient concentrations in ELIS and quantify their influence on biogeochemical transports.

Using model velocities introduces differences from actual conditions. The root-mean-square error between observed and model velocities in ELIS is 0.04 to 0.07 ms^{-1} while the tidal-averaged velocity magnitudes exceed 0.30 ms^{-1} . The average velocities in the outflowing and inflowing layers (approximately 0.2 ms^{-1} for outflow and 0.1 ms^{-1} for inflow over a larger area)

have corresponding standard errors of 2-3% and 3-6% respectively. Uncertainty estimates for ELIS organic carbon exchange fluxes can be found by propagating the errors associated with tidal variability and model velocities. Note that lateral DOC and POC variability cannot be estimated for ELIS with this dataset. The estimated uncertainty is 7-9% for the outward and inward DOC exchange fluxes and 15-16% for the POC exchange fluxes.

Velocity observations do not provide a direct evaluation of the net volume flux (sum of the larger outflowing and inflowing exchange fluxes) because parts of the water column are not measured. However, the long-term net volume flux out of LIS in the model does balance the observed river inflow. This balance indicates broad consistency with the natural system and suggests the relative error of the net volume flux is smaller than for the outward and inward exchange fluxes. Considering only the tidal uncertainty in organic carbon concentrations yields 7% and 15% relative errors in the net DOC and POC fluxes through ELIS. The uncertainty in the modeled outward and inward exchange volume fluxes may create errors in the net carbon flux if there are large vertical (or lateral) variations in concentrations. In ELIS vertical differences in DOC are small and differences in POC are smaller (Figure 3). Including this effect associated with vertical concentrations variations and uncertainty in the exchange volume fluxes increases the estimated uncertainty in net DOC and POC fluxes to at most 14% and 26%, respectively. The highest uncertainties are associated with the 2012 low river flow year. This level of uncertainty remains low enough to distinguish between the carbon export (or import) values reported for different years (as in Figures 4 and 6).

Conclusions

Assessing the role of estuaries in continental shelf carbon budgets is a critical step to improving coastal carbon budgets. There is a general tendency to classify estuaries as either auto or heterotrophic. It is clear from the above analysis that for this temperate estuary, the trophic status and the export of organic carbon varies both seasonally and inter-annually. Based on this assessment of DOC export to the MAB it appears that DOC is delivered to the LIS *from* the MAB during low flow years where freshwater inputs average below $19 \text{ km}^3 \text{ yr}^{-1}$ which represent 15% of the last 20 years. Net DOC flux reverses and delivers DOC to the MAB when river flowrates exceed this threshold. The years in which river flow averages between 19 to $26 \text{ km}^3 \text{ yr}^{-1}$ represent years when the LIS both exports DOC to the MAB and is net heterotrophic. These are the most common conditions for LIS representing 50% of the time period. Finally when river inputs exceed $26 \text{ km}^3 \text{ yr}^{-1}$, LIS is both an exporter of DOC to the MAB and net autotrophic, reflecting a DOC quality that is highly enriched by *in situ* primary production. This latter case applies to 35% of the last 20 years. The DOC export to the MAB (for 1996-2016, with the inter-annual standard deviation) is estimated based on this weighting at $56 \pm 64 \times 10^6 \text{ kg yr}^{-1}$. The temporal trend of freshwater inputs appears to be shifting to relatively high flow conditions and this has important implications for coastal carbon budgets in this and possibly other regions. For LIS the future export impact on the MAB may be increasing. The dependency of trophic status on the inter-annual changes in river flow emphasizes the versatility of these freshwater-saltwater boundaries and raises the concern of not classifying estuaries as solely auto or heterotrophic but instead understanding the dynamic feedbacks to flow conditions and resulting shifts in both the quantity and nature of the OC exported.

Acknowledgments: Funding for this work was provided by Connecticut Sea Grant, University of Connecticut through Award No. NA14OAR4170086, Project Number R/ER-28 and National Science Foundation Grants (Physical Oceanography) 0825812 and 955967. The authors would like to thank John Mullaney of the USGS for data on the freshwater carbon inputs and Matt Lyman of the CT-DEEP.

References

- Abrila, G., Nogueirab, M., Etchebera, H., Cabec, G., Lemairea, E., Brogueirab, M.J. 2002. Behavior of organic carbon in nine contrasting European estuaries. *Estuarine, Coastal and Shelf Science*. 54:241–262.
- Bennett, D. C., O'Donnell, J., Bohlen, W. F., Houk, A. 2010. Tides and overtides in Long Island Sound. *Journal of Marine Research*. 68: 1-35.
- Buck, N.J., Gobler, C.J., Sañudo-Wilhelmy, S.A. 2005. Dissolved trace element concentrations in the east River–long Island Sound system: Relative importance of autochthonous versus allochthonous sources. *Environmental Science & Technology* 39: 3528–3537.
- Cai, W-J. 2011. Estuarine and coastal ocean carbon paradox: CO₂ sinks or sites of terrestrial carbon incineration? *Annu. Rev. Mar. Sci.* 3:123-145.
- Cook T., Folli M., Klinck J., Ford S., Miller J. 1998. The relationship between increasing sea-surface temperature and the northward spread of *Perkinsus marinus* (Dermo) disease epizootics in oysters. *Estuarine, Coastal and Shelf Science*. 46:587-597.

Connecticut Department of Energy and Environmental Protection (CT-DEEP). 2015. 2015 Long Island Sound hypoxia season review.

www.ct.gov/deep/lib/deep/water/lis_water_quality/monitoring/2015/2015_Season_Review_final.pdf

Eppley, R.W., Peterson, B.J. 1979. Particulate organic matter flux and new production in the open ocean. *Nature*. 282:677-680.

Gay, P., O'Donnell, J. 2009. Comparison of the salinity structure of the Chesapeake Bay, the Delaware Bay and Long Island Sound using a linearly tapered advection-dispersion model. *Estuaries and Coasts*. 32: 68-87.

Gobler, C.J., Buck, N.J. Sieracki, M.E., Sañudo-Wilhelmy, S.A. 2006. Nitrogen and silicon limitation of phytoplankton communities across an urban estuary: The East River-Long Island Sound system. *Estuarine, Coastal and Shelf Science*, 68:127-138.

Hopkinson, C. S., B. Fry, and A. Nolin. 1997. Stoichiometry of dissolved organic matter dynamics on the continental shelf of the Northeastern U.S.A. *Continental Shelf Research* 17:473-489.

Jennerjahn, T.C., Knoppers, B.A., deSouza, W.F.L., Carvalho, C.E.V., Mollenhauer, G., Hubner, M., Ittekkot, V. 2010. Tropical Margins. p. 427-442. In, K.K. Liu, L. Atkinson, R. Quiñones, and Talaue-McManus, (Editors) *Carbon and nutrient fluxes in continental margins*. Springer. *Global Change – The IGBP Series*.

Kemp, W.M., Smith, E.M., Marvin-DiPasquale, M., Boynton, W.R. 1997. Organic carbon balance and net ecosystem metabolism in Chesapeake Bay. *Mar Ecol Prog Ser* 150: 229-248.

Koutsikopoulos C., Beillois P., Leroy C., Taillefer F. 1998. Temporal trends and spatial structures of the sea surface temperature in the Bay of Biscay. *Oceanologica Acta*. 21:335-344.

Long Island Sound Study. 1994. Comprehensive conservation and management plan. US Environmental Protection Agency, Long Island Sound Office. Stamford, CT.

http://longislandsoundstudy.net/wp-content/uploads/2010/03/management_plan.pdf

Macdonald, R.W., Anderson, L.G., Christensen, J.P., Miller, L.A., Semiletov, I.P., Stein, R. 2010. Polar Margins. p. 291-302. In, K.K. Liu, L. Atkinson, R. Quiñones, and Talaue-McManus, (Editors) Carbon and nutrient fluxes in continental margins. Springer. Global Change – The IGBP Series.

Mitchell, S.B., Jennerjahn, T.C., Vizzini, S., Zhang, W. 2015. Estuarine, changes to processes in estuaries and coastal waters due to intense multiple pressures – An introduction and synthesis *Coastal and Shelf Science*, 156:1–6.

Mullaney, J.R., 2016. Nutrient, organic carbon and chloride concentrations and loads in selected Long Island Sound tributaries: Four decades of change following the passage of the Federal Clean Water Act. U.S. Geological Survey Scientific Investigations Report 2015–5189, 47 p., <http://dx.doi.org/10.3133/sir20155189>

Najjar, R., Butman, D.E., Cai, W., Friedrichs, M.A.M., Kroeger, K.D., Mannino, A., Raymond, P.A., Salisbury, J., Vandemark, D.C., Vlahos, P. 2010. Carbon budget for the continental shelf of the eastern United States: A Preliminary Synthesis. OCB 3:1-4.

New York State Department of Environmental Conservation and Connecticut Department of Environmental Protection (2000) A total maximum daily load analysis to achieve water-quality standards for dissolved oxygen in Long Island Sound: Albany, N.Y., New York State Department of Environmental Conservation and Hartford, Conn., Connecticut Department of Environmental Protection.

O'Donnell, J. Wilson, R. E., Lwiza, K., Whitney, M. M., Bohlen, W. F., Codiga, D., Fribance, D. B., Fake, T., Bowman, M., Varekamp, J. 2014. The physical oceanography of Long Island Sound. p 125-167. In J.S. Latimer, M.A. Tedesco, R.L. Swanson., C. Yarish and P.E. Stacey [eds], Long Island Sound: Prospects for the Urban Sea. Springer. In Long Island Sound: Prospects for the urban sea, eds. Latimer, J. S., Tedesco, M. A., Swanson, R. L., Yarish, C. and Stacey, P. E., Springer,

Preston B. L. 2004. Observed winter warming of the Chesapeake Bay Estuary (1949–2002): Implications for ecosystem management. Environmental Management. 34:125-139.

Seekell D. A. and Pace M. L. 2011. Climate change drives warming in the Hudson River Estuary, New York (USA). J. Environ. Monit. 13:2321-2327.

Vallino, J.J, Hopkinson, C.S., Garritt, R.H. 2005. Estimating estuarine gross production, community respiration and net ecosystem production: a nonlinear inverse technique. *Ecological Modelling* 187:281–296.

Varekamp, J. C., McElroy, A. E., Mullaney, J. R., Breslin, V. T. 2014. Metals, organic compounds, and nutrients in Long Island Sound: Sources, magnitudes, trends and impacts. p. 250-298. In J.S. Latimer, M.A. Tedesco, R.L. Swanson., C. Yarish and P.E. Stacey [eds], *Long Island Sound: Prospects for the Urban Sea*. Springer.

Vlahos, P., Chen, R. F., Repeta, D. 2002. Fluxes of dissolved organic carbon (DOC) in the Mid-Atlantic Bight. *Deep Sea Research II*. 42:4369-4385.

Walsh, J.J. 1995. DOC storage in Arctic seas: the role of continental shelves. p. 203-230. In W.O. Smith and J.M Grebmeier [eds], *Arctic Oceanography: Marginal ice zones and continental shelves*. Am Geophys Union, Washington DC.

Whitney, M. M., Ullman, D. S., & Codiga, D. L. 2016. Subtidal exchange in eastern Long Island Sound. *Journal of Physical Oceanography*, 46(8): 2351-2371.

Figure Legends

Figure 1. Long Island Sound (LIS) location map including analyzed CT-DEEP stations, LIS regions (WLIS, CLIS, and ELIS), bounding transects (north/south oriented gray lines), Block Island Sound outside the LIS mouth, major rivers, and the East River (a tidal strait) at the LIS head. **Figure 2:** DEEP Station A4 (WLIS) time series data for a) DOC, b) POC, c) DON, d) DIN in (mgL^{-1}), e) C/N (mol/mol).

Figure 2. Carbon and nitrogen time series at CT-DEEP station A4 in WLIS: a) DOC, b) PC, c) DON, d) PN, e) TDN, in (mgL^{-1}), and f) C/N (molmol^{-1}). Near-surface concentrations (thick curves) and near-bottom concentrations (thin curves). Shading indicates the time period when DOC and C/N values appear to have analytical issues.

Figure 3. Along-estuary trends in: a) DOC, b) PC, c) DON, d) PN, e) TDN, in (mgL^{-1}), and f) C/N (mol/mol). Record-averaged values are shown with error bars representing the standard deviation of inter-annual variability. Near-surface concentrations (thick curves) and near-bottom concentrations (thin curves).

Figure 4. Long Island Sound mass balances for a) Low flow conditions (2012) b) High flow condition (2011), $\times 10^6 \text{ kg y}^{-1}$.

Figure 5 LIS *in situ* production values = [productivity – (respiration and burial)] from equation 1 where values are $\times 10^6 \text{ kg y}^{-1}$.

Figure 6. The relationship between river discharge to LIS and net DOC export. The red dashed line defines the transition from net export to net import of DOC from LIS to the adjacent Mid

Atlantic Bight. The solid line defines the transition from net heterotrophic (below) to net autotrophic (above).

Figure 7. Annual LIS River discharge time series with thresholds for net DOC export (dashed line) and net autotrophic (solid line) conditions for LIS.

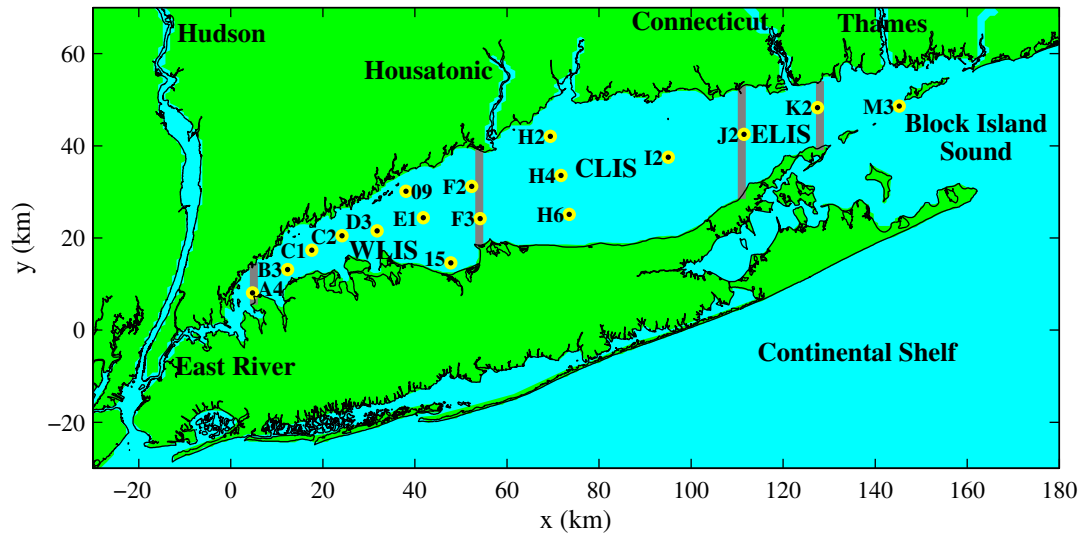


Figure 1 Long Island Sound (LIS) location map including analyzed CT-DEEP stations, LIS regions (WLIS, CLIS, and ELIS), bounding transects (north/south oriented thick lines), Block Island Sound outside the LIS mouth, major rivers, and the East River (a tidal strait) at the LIS head.

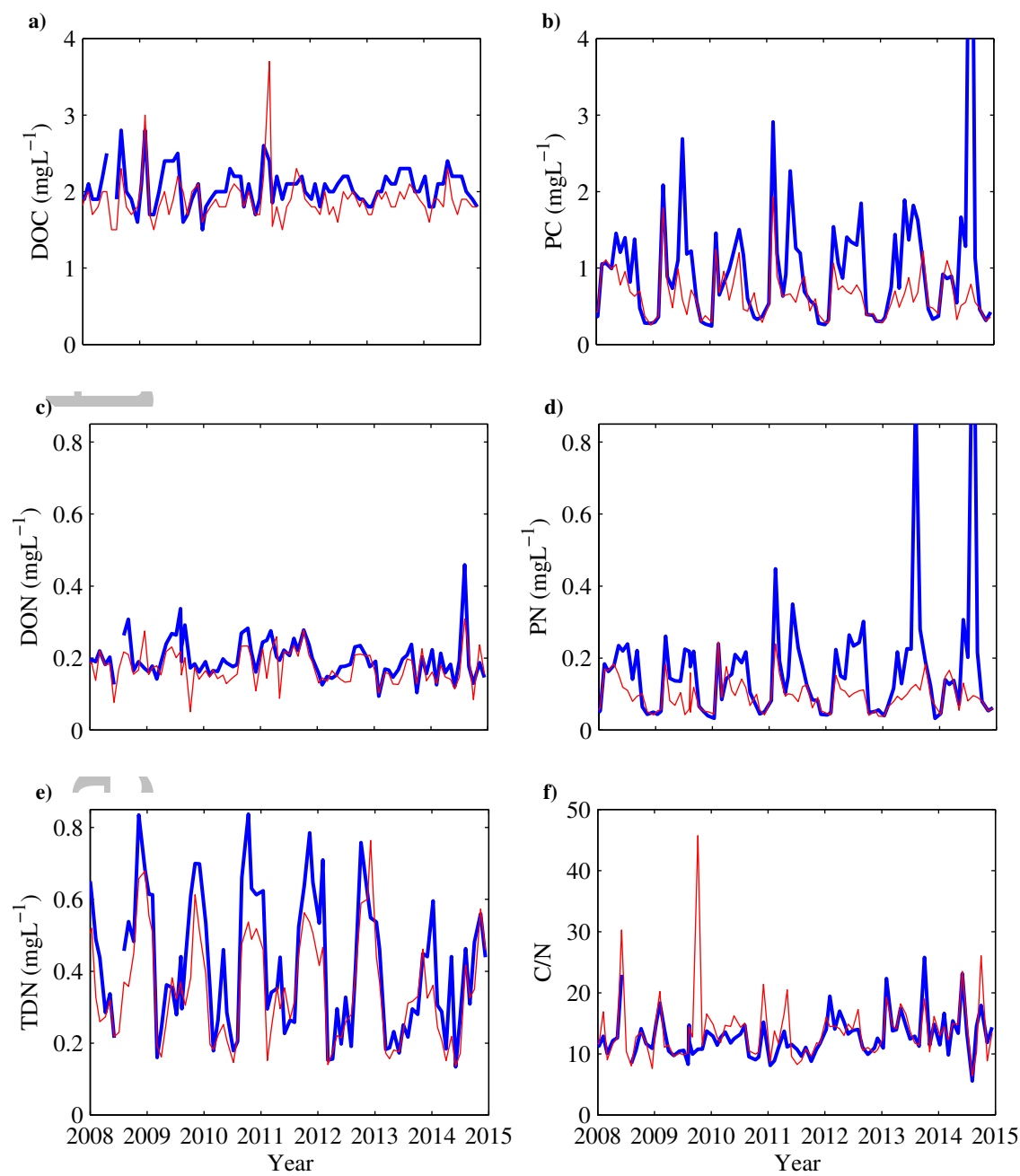


Figure 2 Carbon and nitrogen time series at CT-DEEP station A4 in WLIS: a) DOC, b) PC (a proxy for POC), c) DON, d) PN, e) TDN, and f) C/N. Near-surface concentrations (thick lines) and near-bottom concentrations (thin lines).

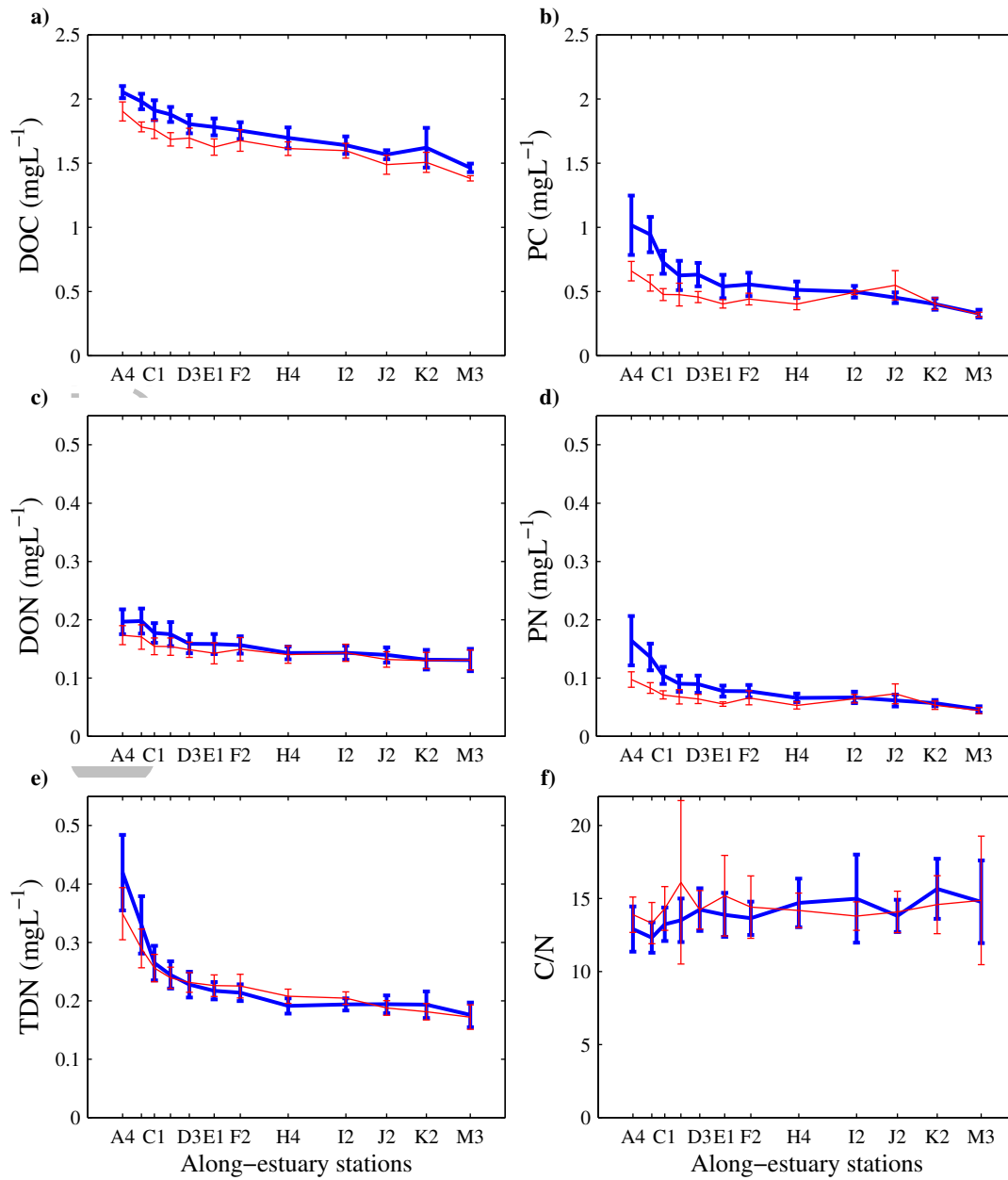
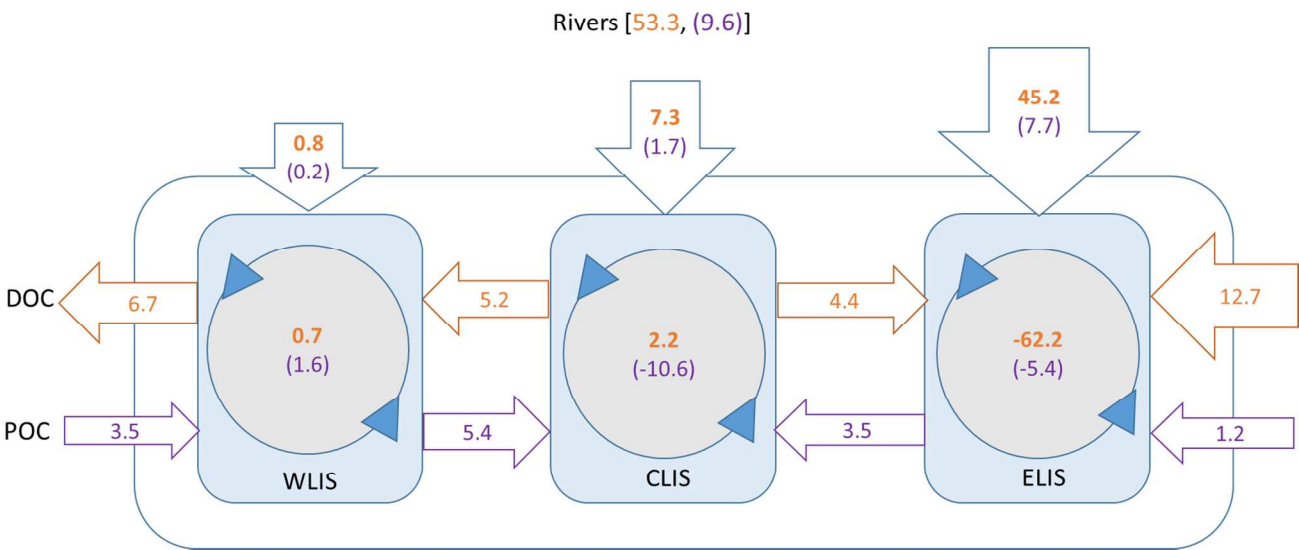


Figure 3 Along-estuary trends in: a) DOC, b) PC (including POC), c) DON, d) PN, e) TDN, and f) C/N. Record-averaged values are shown with error bars representing the standard deviation of inter-annual variability. Near-surface concentrations (thick lines) and near-bottom concentrations (thin lines). Stations spacing is proportional to distance along the estuary.

a) Low Flow Year 2012 (10^6 kg y^{-1})



b) High Flow Year 2011 (10^6 kg y^{-1})

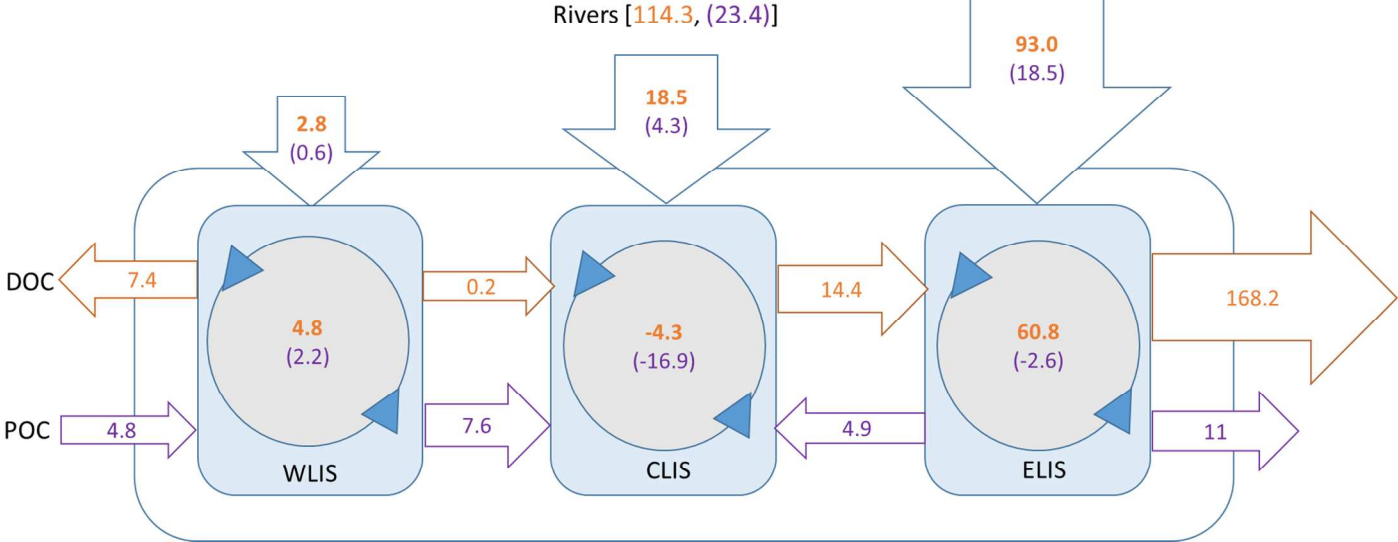


Figure 4 Long Island Sound mass balances for a) Low flow conditions (2012) b) High flow conditions (2011), (10^6 kg y^{-1}).

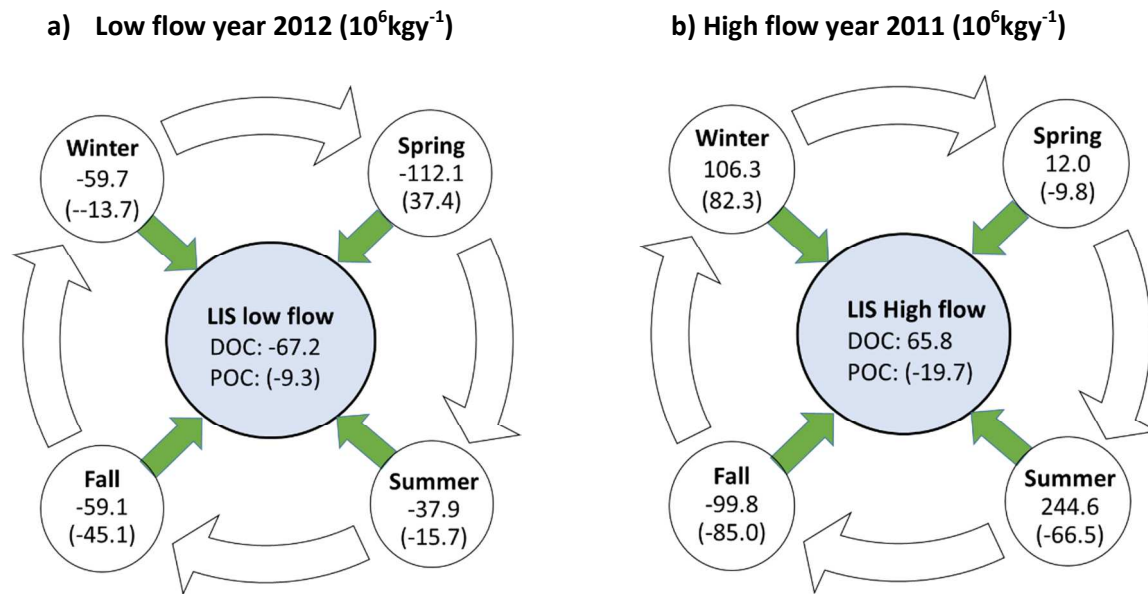


Figure 5 LIS in situ production values = [productivity – (respiration and burial)] from equation 1 where values are $\times 10^6 \text{kgy}^{-1}$.

Accepted

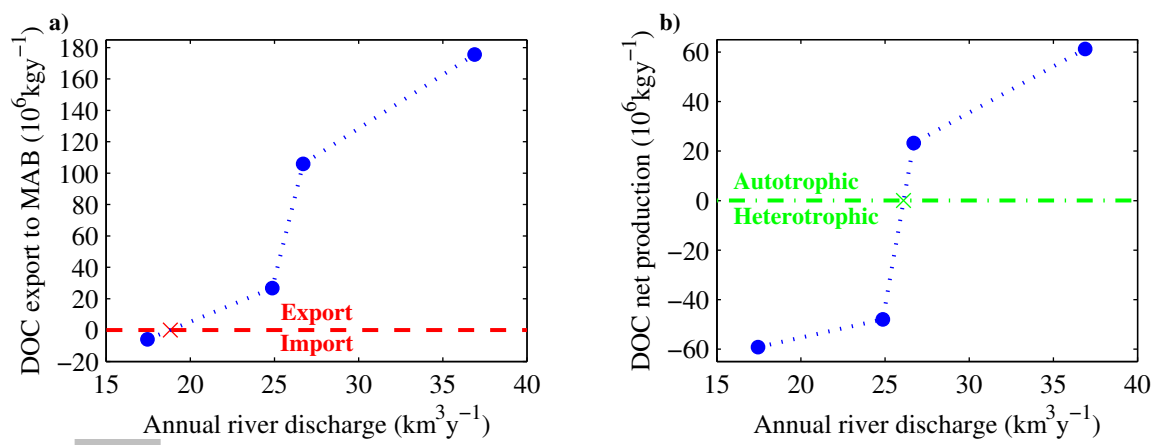


Figure 6 Relationships for a) net DOC export and b) DOC net production vs. river discharge for the LIS budget region. Circles indicate annual results for 2009-2012; dotted lines are connecting linear interpolations. The dashed line is the transition from net export to net import of DOC from LIS to the adjacent Mid Atlantic Bight (MAB). The dashed-dot line is the transition from net autotrophic to heterotrophic conditions. The estimated river discharge corresponding to each threshold is marked with an 'x'.

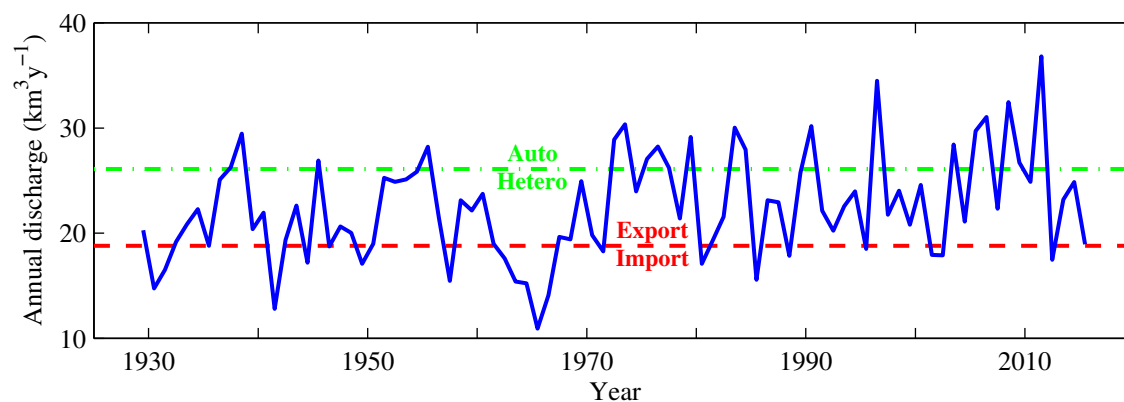


Figure 7 Annual LIS River discharge time series with thresholds for net DOC export (dashed horizontal line) and net autotrophic (dashed-dot horizontal line) conditions for LIS. The thresholds are derived from Figure 6.

Supplemental Information:

Table S1: Timescales Relevant to this Analysis

Time Series	Period
DEEP time series	1995 - ongoing
DEEP data for LIS trends	2008 - 2014
DEEP data for model & budgets	2009 - 2012
USGS Data	
Hydrodynamic model	
Mass balances & Budgets	

Accepted Article

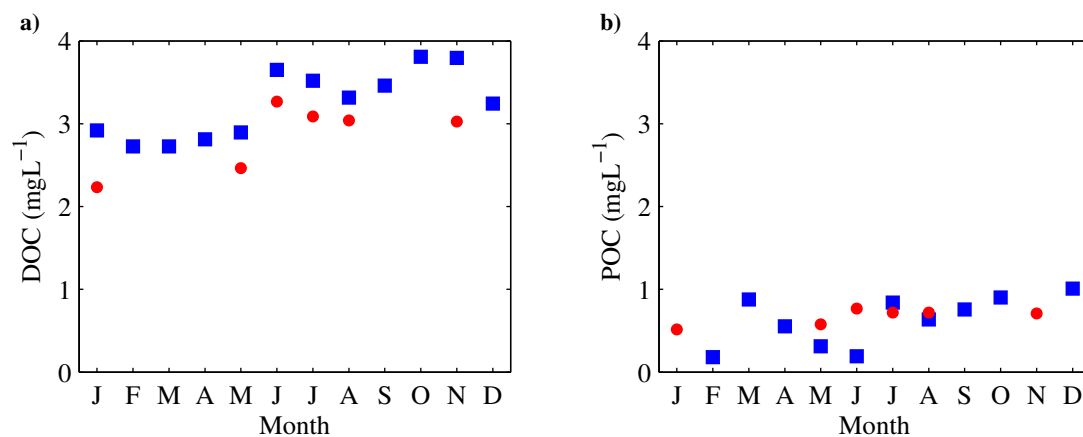


Figure S1 Seasonal cycle for river concentrations of a) DOC and b) POC based on Mullaney (2016). Connecticut River cycle (squares) and Housatonic River cycle (circles) are shown. The Housatonic River cycle is applied to all other rivers.

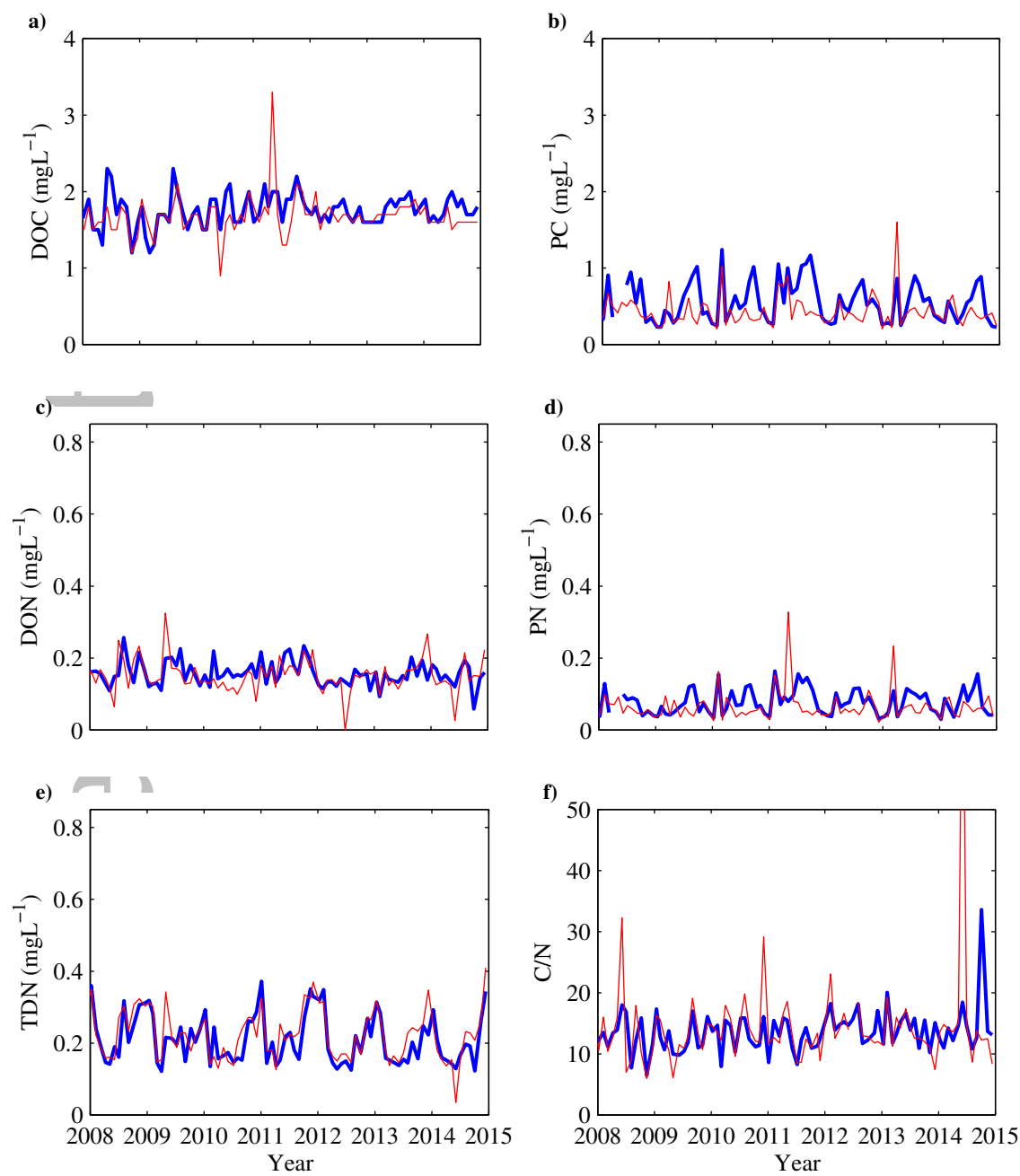


Figure S2 Carbon and nitrogen time series at CT-DEEP station F2 at WLIS/CLIS boundary: a) DOC, b) PC (a proxy for POC), c) DON, d) PN, e) TDN, and f) C/N. Near-surface concentrations (thick lines) and near-bottom concentrations (thin lines).

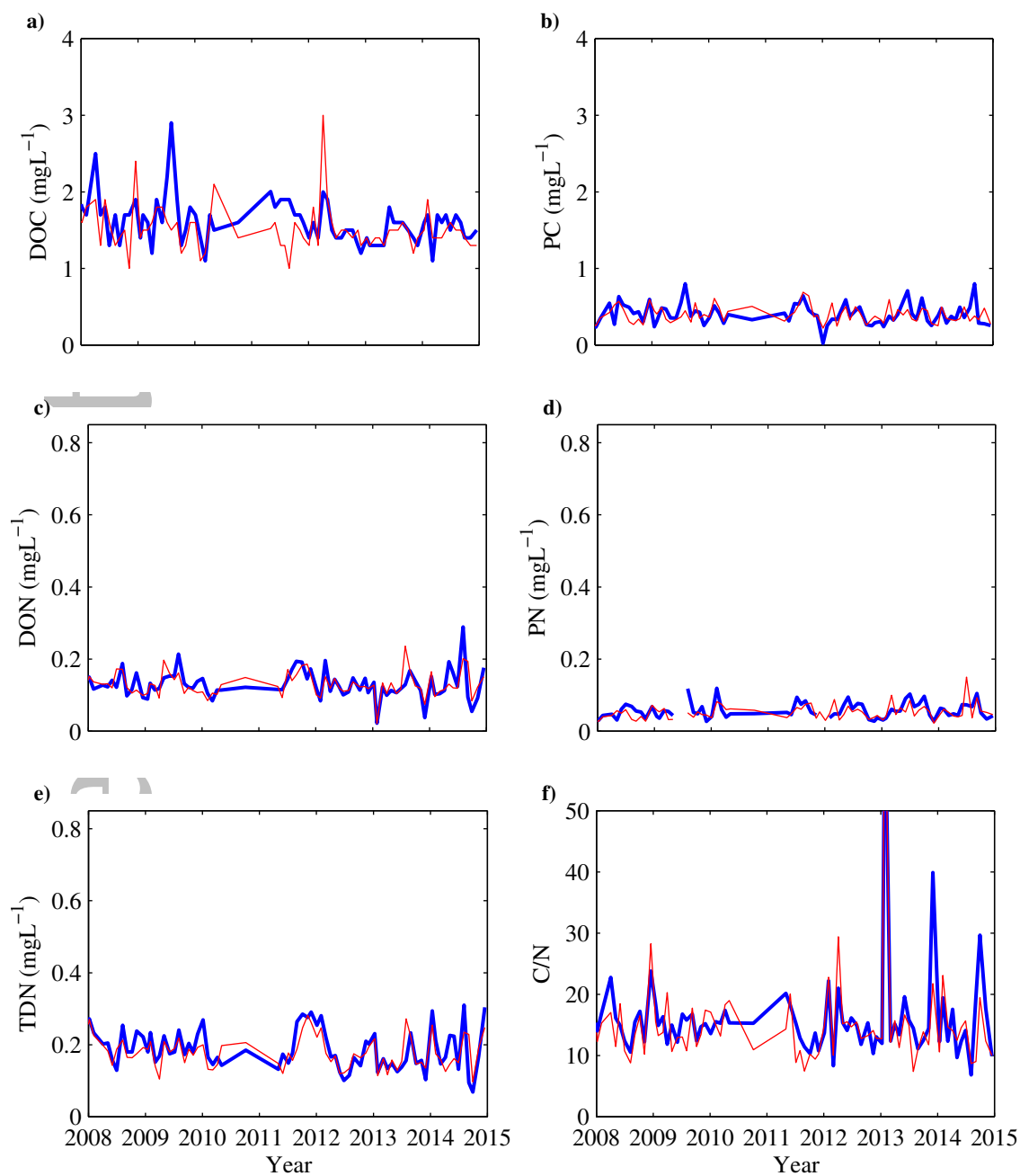


Figure S3 Carbon and nitrogen time series at CT-DEEP station K2 in ELIS: a) DOC, b) PC (a proxy for POC), c) DON, d) PN, e) TDN, and f) C/N. Near-surface concentrations (thick lines) and near-bottom concentrations (thin lines).